

Article

Utilizing Sequential Control Scheme to Stabilize Squeezed Vacuum States

Long Tian ^{1,2} , Xiaocong Sun ¹, Qingwei Wang ¹, Jinrong Wang ¹, Wenxiu Yao ¹, Junping Wang ¹, Yaohui Zheng ^{1,2,*}  and Kunchi Peng ^{1,2}

¹ State Key Laboratory of Quantum Optics and Quantum Optics Devices, Institute of Opto-Electronics, Shanxi University, Taiyuan 030006, China; tianlong@sxu.edu.cn (L.T.); xiaocongsun@163.com (X.S.); qingweiwang1104@163.com (Q.W.); wjrong2017@126.com (J.W.); 18435138386@163.com (W.Y.); wjp201822607022@163.com (J.W.); kcpeng@sxu.edu.cn (K.P.)

² Collaborative Innovation Center of Extreme Optics, Shanxi University, Taiyuan 030006, China

* Correspondence: yzheng@sxu.edu.cn

Received: 13 April 2019; Accepted: 30 April 2019; Published: 7 May 2019



Abstract: We report on a sequential control scheme to realize a steady, quasi-continuous output of squeezed vacuum states, which eliminates the influence of the seed beam on the squeezing strength. The scheme, originating from time-division multiplexing, separates the generation process from the locking process. We confirm that the sequential control scheme does not reduce the squeezing strength and that the setup operates stably for a 3-h running test, with a duty ratio of 80% and cycle time of 5 s. Therefore, the sequential control scheme opens up a new path of manipulating squeezed vacuum states.

Keywords: squeezed vacuum states; subthreshold optical parametric oscillator; sequential control scheme

1. Introduction

Squeezed states are one of the most principal non-classical states of light in the continuous-variable regime, which were first considered to exist in the 1920s by Schrödinger, Kennard, and Darwin [1–3]. In 1981, Caves proposed that squeezed states can be used to surpass the quantum limit in an interferometric gravitational wave detector by injecting squeezed states into the dark port of the interferometer [4]. In addition, the squeezed state can be also used to realize quantum imaging [5,6] beyond the diffraction limit [7], spectroscopic measurement [8], velocimetry [9], and LIDAR [10] and generate a Schrödinger cat state and an Einstein–Podolsky–Rosen state for continuous-variable quantum information [11–15]. All these applications require squeezed states with a high-level and stable squeezing strength.

Squeezed states can be generated by using an optical parametric oscillator (OPO) based on second-order nonlinearity [16], four-wave mixing based on third-order nonlinearity [17], and other schemes [18]. Using an OPO is one of the most successful methods of squeezed state generation, which also holds the record of the squeezing level [19]. The first experimental demonstration of a squeezed state based on the OPO was performed in 1986 [16]. In ideal conditions, an infinite squeezing factor can be generated and detected at the threshold. However, the non-ideal components introduce an inevitable loss during the generation, propagation, and detection of the squeezed states, and the actual servo-loops have inherent noise and drift that result in phase fluctuation during the cavity- and phase-locking [19–30]. A monolithic cavity with the least number of optical surfaces can effectively reduce the intracavity losses [31–34]. The primary advantage of a doubly-resonant OPO cavity over a single-resonant OPO cavity is the simplicity of obtaining a cavity error signal by using

the pump field. That means the pump field amplitude is resonantly enhanced and allows increasing the transmission of the output coupler for increasing the escape efficiency. The doubly-resonant OPO cavity has other advantages including lower pump power, perfect mode matching, and so on. However, the doubly-resonant OPO cavity needs more stringent temperature stability requirements for simultaneously realizing co-resonance and best phase matching. The photothermal effect associated with absorption of the pump field in a doubly-resonant OPO cavity may be more serious than a single-resonant OPO cavity. A semi-monolithic OPO cavity has an external piezo-driven coupling mirror that can be used to impose the feedback control signal. This is a more popular scheme [19,24,25,35,36], and it has been applied to squeezed states' generation with a high-level squeezing factor [19]. The error signal for OPO locking can be extracted from the pump field in the case of a double-resonant cavity [36]. A single-resonant cavity has a single- or double-pass configuration for the pump field, which makes it unsuitable for the locking scheme to extract the error signal from the pump field. During the generation of bright squeezed light, the seed beam injected into the OPO makes the control of the cavity length and relative phase simple [25]. In this case, a seed beam injected into the optical parametric amplifier (OPA) dramatically degenerates the squeezing factor due to noise coupling between the pump and seed fields, even if both the pump and seed fields have no classical noise [37]. As the analysis frequency decreases, the limit factor becomes significant due to the increase of laser intensity noise, until squeezing can no longer be achieved [30].

The generation of squeezed vacuum states eliminates noise coupling between the pump and seed beam, which enables the production of a high-level squeezing factor that is immune to laser noise. However, there is no coherent seed beam injected into the OPO, which serves as a locking beam. Thus, there is no direct way to extract the error signals of locking the single-resonant cavity length and relative phase. Therefore, squeezed vacuum states are usually generated by manually scanning the bias voltage imposed on the piezo-driven coupling mirror over the OPO cavity resonance. Its drawback is the lack of stability, and hence, it cannot meet the requirement for practical applications. By employing a quantum noise locking scheme [38] or using two additional coherent, but frequency-shifted auxiliary beams to control the cavity length and relative phase, long-term stable squeezed vacuum states can be achieved [39]. The scheme is derived from frequency-division multiplexing ideas.

In this paper, we realize a steady quasi-continuous output of squeezed vacuum states by utilizing a sequential control scheme that was derived from time-division multiplexing ideas [40,41], which operate an independent signal at different time periods. The control algorithm was managed by a self-designed program compiled on a field programmable gate array (FPGA) hardware platform. The operation process was divided into ready mode and carry mode. In ready mode, the locking beam (seed beam) has a coherent amplitude that can be used to extract the error signal for cavity- and phase-locking, generating a bright squeezed state. In carry mode, the voltage hold circuit starts working, and the locking beam is blocked, generating squeezed vacuum states. The presence of a locking beam reduces the squeezing strength due to classical noise coupling between the pump and locking beams, and it worsens below the MHz range. The sequential control scheme, originating from time-division multiplexing, can realize the stable generation of squeezed vacuum states within a certain period of time without the locking beam, which eliminates the influence of noise coupling between the pump and locking beams on the squeezing strength in carry mode. The measured non-classical noise reduction of squeezed vacuum states was 11.6 dB and 10.4 dB at the analysis frequencies of 2 MHz and 500 kHz, respectively. The setup operated stably for a 3-h running test, with an 80% duty ratio and 5-s cycle time. The stable quasi-continuous generation of high-level squeezed vacuum states has great significance in practical quantum systems.

2. Experimental Setup

The schematic of our experimental setup is shown in Figure 1. We used a home-made single-frequency Nd:YVO₄ laser at 1064 nm as the laser source. A Faraday isolator (FI) was inserted between the laser and OPO to reduce the backscatter disturbance. Three mode cleaners (MC) were

used not only to provide spatial-temporal filtering and polarization purifying for the downstream experiment, but also as an auxiliary cavity for high-efficiency mode-matching. The majority of the laser power was frequency doubled in a second harmonic generator (SHG) to produce a pump beam of up to 600 mW for the parametric downconversion processes. We actually used a 90:10 beamsplitter to split a fraction of the laser to use as the local beam. A half wave plate and a polarization beamsplitter (not shown in the figure) were also used to adjust the power of the local beam.

Our OPO was a semi-monolithic cavity consisting of a piezo-actuated concave mirror and a periodically poled potassium titanyl phosphate (PPKTP) crystal with dimensions of $1\text{ mm} \times 2\text{ mm} \times 10\text{ mm}$. The crystal end face with a curvature radius of 12 mm was coated for high-reflection (HR) for the fundamental beam and high-transmission (HT) for the pump beam, thus serving as one of the cavity mirrors. The plane front face of the crystal was coated for antireflection (AR) for both wavelengths. An air gap of 26 mm existed between the AR-coated side of the crystal and the coupling mirror. The concave mirror with a radius of curvature of 30 mm had a transmissivity of 12% for 1064 nm and HR for 532 nm, and it was used as the output coupler. The squeezed vacuum states interfered with an local oscillator (LO) on a 50:50 beamsplitter. The output beam from the 50:50 beamsplitter was directed towards a balanced homodyne detector (BHD) to detect the noise level. In our setup, the optical path was as short as possible, aiming to minimize the phase drift over the experiment, and the distance between OPO (1064MC2) and the 50:50 beamsplitter was about 10 (16) cm.

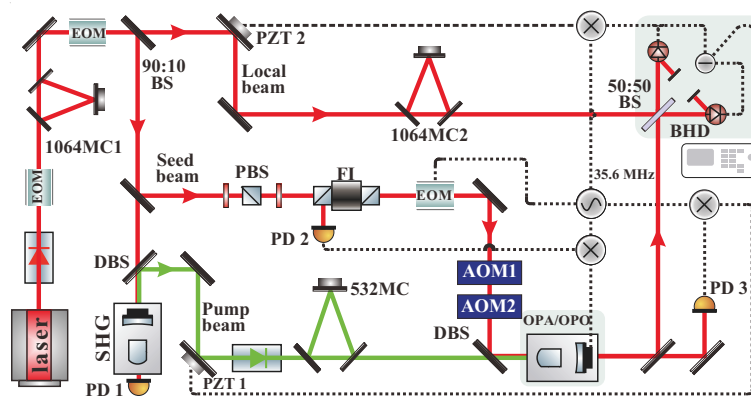


Figure 1. Schematic of the experimental setup. The seed beam was switched on/off by two AOMs manipulated by an FPGA. Laser: single-frequency Nd:YVO₄ laser; EOM, electro-optic modulator; AOM, acousto-optic modulator; FI, Faraday isolator; MC, mode cleaner; SHG, second harmonic generator; OPO, optical parametric oscillator; OPA, optical parametric amplifier; DBS, dichroic beamsplitter; BS, beamsplitter; PBS, polarization beamsplitter; PZT1-2, piezoelectric transducer; PD1-3, photodetector; BHD, balanced homodyne detector.

The squeezed light emitting from the concave mirror was separated from the pump light by a dichroic beamsplitter and directed towards a BHD to detect the noise level. The BHD, with a common mode rejection ratio of 75 dB [42–44], was built from a pair of p–i–n semiconductor structure (PIN) photodiodes (Laser Components, Germany) with a quantum efficiency of more than 99%.

The phase modulation signal, having a frequency of 35.6 MHz, was imprinted on the locking beam to generate error signals for all three control loops [45,46]: the error signal for stabilizing the OPA cavity length on resonance was demodulated from the output of the photodetector PD3; the error signal of locking the relative phase between the pump and the signal beams was obtained from the photodetector PD2 placed at the reflected end of the OPA, and the relative phase between the LO beam and signal beam was locked by demodulating the output signal of the homodyne detector and feeding back to the piezoelectric transducer PZT2 on the optical path of the LO beam. When the lock power

was less than 15 mW, the amplitude of the error signal was insufficient to obtain a stable locking for the OPA cavity and relative phase.

It is worth mentioning that two acousto-optic modulators (AOMs), which were driven at the same frequency, were inserted before the OPO in our experimental setup to switch on/off the locking beam. The first-order diffracted light of AOM1 was the incident beam of AOM2, and the -1 -order diffracted light of AOM2 served as the locking beam. We used two AOMs, not only to reduce the undesired scattered light, but also to make the locking beam have the same mode as the squeezed vacuum state. The two AOMs were manipulated by a self-designed control sequence compiled on an FPGA hardware platform. In ready mode, the presence of a locking beam allowed direct photocurrent detection to extract the error signal of the cavity and phase locking. Before switching to the carry mode, a hold circuit was activated to maintain the voltage for driving the piezoelectric transducer (PZT), leaving the system in the expected state. Subsequently, the locking beam was switched off under FPGA control, and stable squeezed vacuum states were obtained. After a period of operation, the system was switched to ready mode. The locking beam was blocked using two AOMs; the hold circuit was discharged, and the system looked for a new operation state.

3. FPGA Implementation of Sequential Control Scheme

To realize steady squeezed states, at least three servo-control loops are necessary: OPO cavity length, relative phase between the pump and seed beams, and relative phase between the LO and seed beam. The seed beam, namely the locking beam in our setup, served as a mediator for phase stabilization between the pump beam and LO. The block diagram of the sequential control scheme is shown in Figure 2. During initialization, the operation process was similar to that of bright squeezed state generation [25]. The locking beam (seed beam) had a coherent amplitude that could be used to extract the error signals for cavity- and phase-locking. With the initialization complete, the system was switched to carry mode. In carry mode, the voltage hold circuits started working, and the locking beam was blocked. Owing to the design of the quasi-monolithic OPO and short optical path, the setup was stable at the timescale of several seconds without the servo-control loop. Thus, the OPO cavity and two relative phases maintained the same working status as the ready mode within a certain period of time. In the meantime, squeezed vacuum states were stably generated. After the period of work, the locking beam was switched on, the voltage hold circuit stopped working, and the system was switched to ready mode. In ready mode, the system was again recovered to the optimal status with the aid of the locking beam, which was better prepared for the next carry mode.

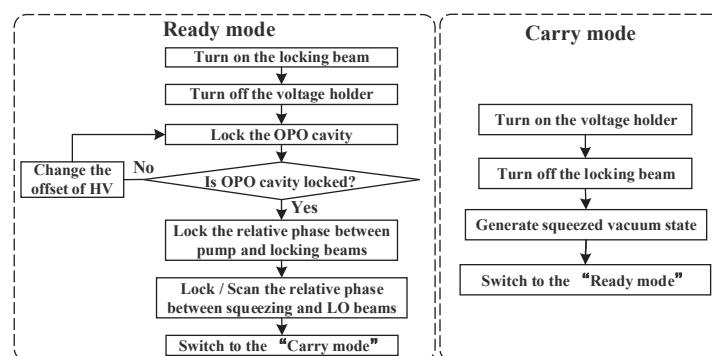


Figure 2. Block diagram of the FPGA-based algorithm. LO, local oscillator; HV, high voltage.

The time sequence of the locking scheme is shown in Figure 3. We used an FPGA-based hardware platform to generate the time sequence and control the output signal. The on-off action of the locking beam was actuated by two AOMs. The voltage holder confirmed that the driving voltage imposed on the PZT remained unchanged during the time of no locking beam, until the next locking pulse arrived. After the arrival of the next locking pulse, three servo-control loops were activated, whereas the

voltage hold circuits were disabled. The spectrum analyzer operated in gate mode to synchronize the measurement process. To perform the complete measurement process, the LO phase operated in three modes: one was locked to zero with respect to the locking beam to measure quadrature amplitude component; the second was locked to $\pi/2$ with respect to the locking beam to measure quadrature phase component; the third was scanning mode.

The time sequence described above was realized by virtue of the self-designed operation control program, which was compiled on an FPGA hardware platform. The sequential control scheme, based on the FPGA platform, can be extended to the generation of multipartite entangled states, and the number of its control loops presented a linear increase with the increase of the dimension of the state [47,48].

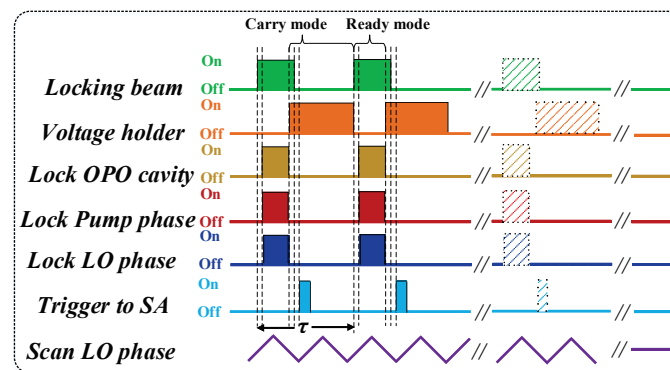


Figure 3. Time sequence of the experimental cycle. SA, spectrum analyzer.

4. Experimental Process and Results

The threshold power of our OPO was 160 mW. First, we measured the squeezing strength of squeezed vacuum states without the locking beam by manually applying offset voltage to the piezo, which was attached to the output mirror of the OPO. The best squeezing factor, recorded by a spectrum analyzer (FSW8 with 0.2 dB uncertainty, Rohde & Schwarz, Germany) was 11.6 dB at the analysis frequency of 2 MHz. The total LO power before the beamsplitter was 5.5 mW, corresponding to the dark noise clearance of 28 dB [49]. Subsequently, we repeated the above measurement with the locking beam power of 50 mW, corresponding to the quantum noise reduction of 10 dB. While the above data were collected, no experimental parameters other than the locking beam being injected were varied. The squeezing factor degradation originated from the noise coupling between the pump and locking beams.

Then, we performed the above measurements again with the sequential control scheme. The measured results are shown in Figure 4; the discontinuity along the time axis corresponds to the switchover point from carry mode to ready mode. Trace (a) corresponds to the shot-noise limit of 5.5 mW LO power. Trace (b) and trace (c) are, respectively, the squeezing and anti-squeezing factors at the pump power of 125 mW. Trace (d) is the measured noise level with the LO phase scanned. The generation of squeezed vacuum states corresponds to carry mode; the squeezing factor was 11.6 dB. Moreover, a bright squeezed state was generated in ready mode with the squeezing factor of 10 dB. These results are in good agreement with those without the sequential control scheme. The cycle time and duty ratio of the time sequence were 2 s and 50%, respectively. Carry mode lasted for 1 s, and the ready process also lasted for 1 s. The squeezing factor in carry mode was independent of the locking beam and without the need for manual control. Therefore, the sequential control scheme opens up a new path of manipulating squeezed vacuum states based on the idea of time-division multiplexing.

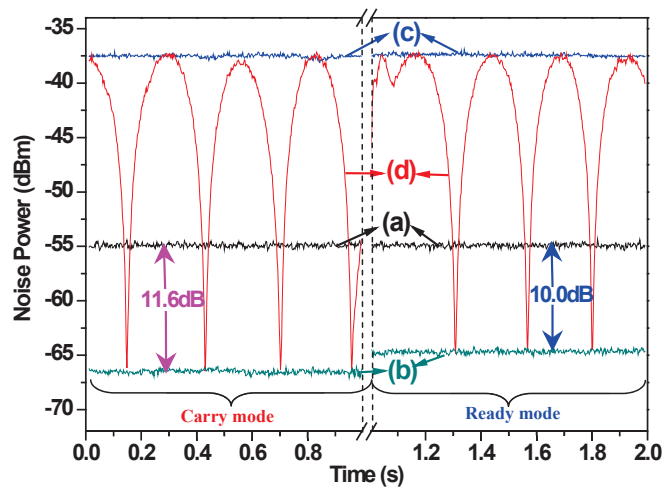


Figure 4. Balance homodyne measurements of the quadrature noise variances with the sequential control scheme. The measurement was recorded at a Fourier frequency of 2 MHz, with an resolution bandwidth (RBW) of 300 kHz and a video bandwidth (VBW) of 200 Hz. The data represent direct observations and contained electronic noise.

We repeated the above experimental process at a Fourier frequency of 500 kHz. First, we independently measured the quadrature noise variances of the squeezed vacuum state and bright squeezed state. The squeezing factor of the squeezed vacuum states was 10.4 dB, while the squeezing strength disappeared for the bright squeezed state. Then, we continuously measured the quadrature noise variances by utilizing the sequential control scheme, which is shown in Figure 5. Trace (a) corresponds to the shot-noise limit of 5.5 mW LO power and was measured with the squeezed light blocked. Trace (b) and trace (c) are the squeezing and anti-squeezing factors with the LO phase locked at the pump power of 125 mW. Trace (d) is a noise level with the LO phase scanned. It is worth noting that the squeezing factor reduced to 0 dB with the locking beam at the analysis frequency of 500 kHz, which can be attributed to the increase of laser intensity noise with the decrease of analysis frequency. The results further demonstrate the significance of the sequential control scheme, especially for squeezed state generation below the MHz range.

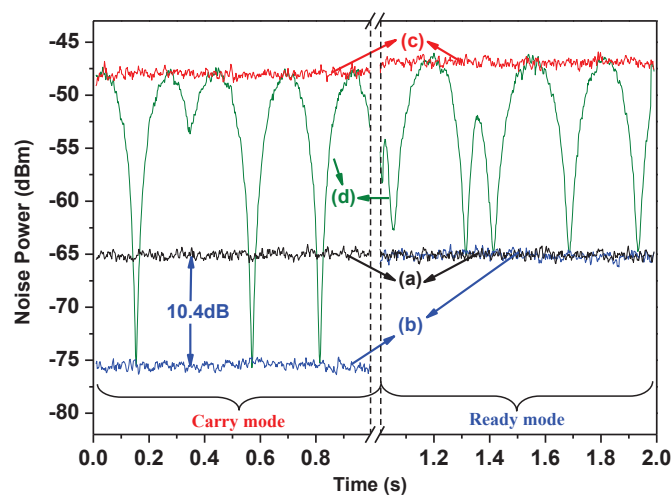


Figure 5. Balance homodyne measurements of the quadrature noise variances at a Fourier frequency of 500 kHz, with an RBW of 10 kHz and a VBW of 20 Hz. The data contained electronic noise and represent direct observations.

To evaluate the long-term stability of the generated squeezed vacuum states, the quadrature noise variances of the squeezed state at the pump power of 125 mW (2 MHz) were recorded continuously for 3 h by utilizing the sequential control scheme. The cycle time and duty ratio of the time sequence were set to 5 s and 80%, respectively. Carry mode lasted for 4 s, and ready mode lasted for 1 s. The long-term stability results are shown in Figure 6, which confirms that the control scheme can realize the steady, quasi-continuous output of squeezed vacuum states.

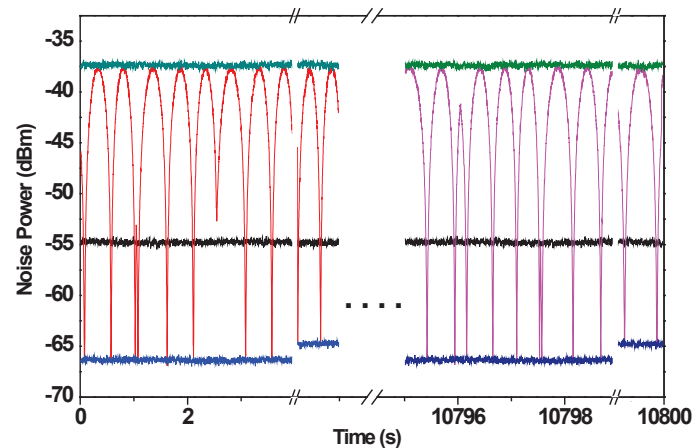


Figure 6. Long-term stability of the squeezed vacuum states of light recorded continuously for 3 h, with an RBW of 300 kHz, a VBW of 200 Hz, and a gate time of 3 h.

5. Conclusions

In conclusion, owing to the design of the quasi-monolithic OPO and short optical path, the setup was stable at the timescale of several seconds without the servo-control loop. In combination with a sequential control scheme compiled on an FPGA hardware platform, we realized a steady, quasi-continuous output of squeezed vacuum states. In the case with the seed beam (locking beam), the system operated in ready mode; the cavity length and relative phases were actively locked to the desired state. In the case without the seed beam, it operated in carry mode; squeezed vacuum states were stably generated during the follow-up period of blocking the seed beam. The setup operated stably for a 3-h running test, with a duty ratio and cycle time of 80% and 5 s, respectively. Therefore, the sequential control scheme opens up a new path of manipulating squeezed vacuum states, which has great significance in practical quantum systems. The sequential control scheme, based on the FPGA platform, can be extended to the generation of multipartite entangled states, which require more servo-control loops.

Author Contributions: Y.Z. and L.T. conceived and designed the experiment. L.T., X.S. and Q.W. carried out the experiment. All authors analysed the data. Y.Z. and L.T. wrote the paper. Y.Z. supervised the whole project.

Funding: National Natural Science Foundation of China (NSFC) (Grant No.11654002, 61575114, 11874250 and 11804207); National Key Research and Development Program of China (2016YFA0301401); Program for Sanjin Scholar of Shanxi Province; Program for Outstanding Innovative Teams of Higher Learning Institutions of Shanxi; Fund for Shanxi “1331 Project” Key Subjects Construction; Natural Science Foundation of Shanxi Province, China, under Grant 201801D221006.

Conflicts of Interest: The authors declare no conflicts of interest.

References

1. Schrödinger, E. Der stetige Übergang von der Mikro-zur Makromechanik. *Naturwissenschaften* **1926**, *14*, 664. [[CrossRef](#)]
2. Kennard, E.H. Zur Quantenmechanik einfacher Bewegungstypen. *Zeitschrift für Physik* **1927**, *44*, 326. [[CrossRef](#)]
3. Darwin, C.G. Free motion in the wave mechanics. *Proc. R. Soc. Lond. Ser. A* **1927**, *117*, 258. [[CrossRef](#)]

4. Caves, C.M. Quantum-mechanical noise in an interferometer. *Phys. Rev. D* **1981**, *23*, 1693. [[CrossRef](#)]
5. Kolobov, M.I.; Kumar, P. Sub-shot-noise microscopy: Imaging of faint phase objects with squeezed light. *Opt. Lett.* **1993**, *18*, 849. [[CrossRef](#)]
6. Lu, B.Z.; Feng, S.W.B.; Kang, M.H.; Qin, F. Experimental Study on the Imaging of the Squeezed State Light with -4.93 dB Quantum-Noise Reduction at 1064 nm. *Adv. Mater. Res.* **2012**, *571*, 439. [[CrossRef](#)]
7. Taylor, M. Subdiffraction-Limited Quantum Imaging of a Living Cell. In *Quantum Microscopy of Biological Systems*; Springer International Publishing: Berlin/Heidelberg, Germany, 2015; p. 153.
8. Polzik, E.S.; Carri, J.; Kimble, H.J. Spectroscopy with squeezed light. *Phys. Rev. Lett.* **1992**, *68*, 3020. [[CrossRef](#)]
9. Li, Y.Q.; Lynam, P.; Xiao, M.; Edwards, P.J. Sub-shot-noise laser Doppler anemometry with amplitude-squeezed light. *Phys. Rev. Lett.* **1997**, *78*, 3105. [[CrossRef](#)]
10. Dutton, Z.; Shapiro, J.H.; Guha, S. LADAR resolution improvement using receivers enhanced with squeezed-vacuum injection and phase-sensitive amplification. *J. Opt. Soc. Am. B* **2010**, *27*, 63. [[CrossRef](#)]
11. Gottesman, D.; Preskill, J. Secure quantum key distribution using squeezed states. In *Quantum Information with Continuous Variables*; Springer: Dordrecht, The Netherlands, 2003; p. 317.
12. Feng, J.; Wan, Z.; Li, Y.; Zhang, K. Distribution of continuous variable quantum entanglement at a telecommunication wavelength over 20 km of optical fiber. *Opt. Lett.* **2017**, *42*, 3399. [[CrossRef](#)] [[PubMed](#)]
13. Huo, M.; Qin, J.; Cheng, J.; Yan, Z.; Qin, Z.; Su, X.; Peng, K. Deterministic quantum teleportation through fiber channels. *Sci. Adv.* **2018**, *4*, eaas9401. [[CrossRef](#)] [[PubMed](#)]
14. Kaiser, B.F.F.; Zavatta, A.; Auria, V.D.; Tanzilli, S. A fully guided-wave squeezing experiment for fiber quantum networks. *Optica* **2016**, *3*, 362. [[CrossRef](#)]
15. Ourjoumtsev, A.; Tualle-Brouiri, R.; Laurat, J.; Grangier, P. Generating optical Schrödinger Kittens for quantum information processing. *Science* **2006**, *312*, 83. [[CrossRef](#)] [[PubMed](#)]
16. Wu, L.A.; Kimble, H.J.; Hall, J.L.; Wu, H.F. Generation of squeezed states by parametric down conversion. *Phys. Rev. Lett.* **1986**, *57*, 2520. [[CrossRef](#)] [[PubMed](#)]
17. Slusher, R.E.; Hollberg, L.W.; Yurke, B.; Mertz, J.C.; Valley, J.F. Observation of squeezed states generated by four-wave mixing in an optical cavity. *Phys. Rev. Lett.* **1985**, *55*, 2409. [[CrossRef](#)] [[PubMed](#)]
18. Yurke, B. Squeezed-state generation using a Josephson parametric amplifier. *J. Opt. Soc. Am. B* **1987**, *4*, 1551. [[CrossRef](#)]
19. Vahlbruch, H.; Mehmet, M.; Danzmann, K.; Schnabel, R. Detection of 15 dB Squeezed States of Light and their Application for the Absolute Calibration of Photoelectric Quantum Efficiency. *Phys. Rev. Lett.* **2016**, *117*, 110801. [[CrossRef](#)]
20. Takeno, Y.; Yonezawa, H.; Furusawa, A. Observation of -9 dB quadrature squeezing with improvement of phase stability in homodyne measurement. *Opt. Express* **2007**, *15*, 4321. [[CrossRef](#)]
21. Stefszky, M.S.; Mow-Lowry, C.M.; Chua, S.S.; Shaddock, D.A.; Buchler, B.C.; Vahlbruch, H.; Khalaidovski, A.; Schnabel, R.; Lam, P.K.; McClelland, D.E. Balanced homodyne detection of optical quantum states at audio-band frequencies and below. *Class. Quant. Grav.* **2012**, *29*, 145015. [[CrossRef](#)]
22. Eberle, T.; Steinlechner, S.; Bauchowitz, J.; Handchen, V.; Vahlbruch, H.; Mehmet, M.; Müller-Ebhardt, H.; Schnabel, R. Quantum enhancement of the zero-area sagnac interferometer topology for gravitational wave detection. *Phys. Rev. Lett.* **2010**, *104*, 251102. [[CrossRef](#)] [[PubMed](#)]
23. Vahlbruch, H.; Mehmet, M.; Chelkowski, S.; Hage, B.; Franzen, A.; Lastzka, N.; Schnabel, R. Observation of squeezed light with 10-dB quantum-noise reduction. *Phys. Rev. Lett.* **2008**, *100*, 033602. [[CrossRef](#)]
24. Shi, S.; Wang, Y.; Yang, W.; Zheng, Y.; Peng, K. Detection and perfect fitting of 13.2 dB squeezed vacuum states by considering green-light-induced infrared absorption. *Opt. Lett.* **2018**, *43*, 5411. [[CrossRef](#)]
25. Yang, W.; Shi, S.; Wang, Y.; Ma, W.; Zheng, Y.; Peng, K. Detection of stably bright squeezed light with the quantum noise reduction of 12.6 dB by mutually compensating the phase fluctuations. *Opt. Lett.* **2017**, *42*, 4553. [[CrossRef](#)]
26. Schneider, K.; Lang, M.; Mlynek, J.; Schiller, S. Generation of strongly squeezed continuous-wave light at 1064 nm. *Opt. Express* **1998**, *2*, 59. [[CrossRef](#)]
27. Serikawa, U.; Yoshikawa, J.I.; Makino, K.; Frusawa, A. Creation and measurement of broadband squeezed vacuum from a ring optical parametric oscillator. *Opt Express* **2016**, *24*, 28383. [[CrossRef](#)]
28. Morin, O.; Liu, J.; Huang, K.; Barbosa, F.; Fabre, C.; Laurat, J. Quantum state engineering of light with continuous-wave optical parametric oscillators. *J. Vis. Exp.* **2016**, *87*, e51224. [[CrossRef](#)]

29. Dwyer, S.; Barsotti, L.; Chua, S.S.; Evans, M.; Factourovich, M.; Gustafson, D.; Isogai, T.; Kawabe, K.; Khalaidovski, A.; Lam, P.K.; et al. Squeezed quadrature fluctuations in a gravitational wave detector using squeezed light. *Opt. Express* **2013**, *21*, 19047. [[CrossRef](#)]
30. McKenzie, K.; Grosse, N.; Bowen, W.P.; Whitcomb, S.E.; Gray, M.B.; McClelland, D.E.; Lam, P.K. Squeezing in the audio gravitational wave detection band. *Phys. Rev. Lett.* **2004**, *93*, 161105. [[CrossRef](#)]
31. Ast, S.; Mehmet, M.; Schnabel, R. High-bandwidth squeezed light at 1550 nm from a compact monolithic PPKTP cavity. *Opt. Express* **2013**, *21*, 13572. [[CrossRef](#)]
32. Yonezawa, H.; Nagashima, K.; Furusawa, A. Generation of squeezed light with a monolithic optical parametric oscillator: Simultaneous achievement of phase matching and cavity resonance by temperature control. *Opt. Express* **2010**, *18*, 20143. [[CrossRef](#)]
33. Zielinska, J.A.; Mitchell, M.W. Atom-resonant squeezed light from a tunable monolithic ppRKTP parametric amplifier. *Opt. Lett.* **2018**, *43*, 643. [[CrossRef](#)]
34. Zielinska, J.A.; Zukauskas, A.; Canalias, C.; Noyan, M.A.; Mitchell, M.W. Fully-resonant, tunable, monolithic frequency conversion as a coherent UVA source. *Opt Express* **2017**, *25*, 1142. [[CrossRef](#)] [[PubMed](#)]
35. Yao, L.; Feng, J.; Gao, Y.; Zhang, K. Generation of a low-frequency squeezed states at telecommunication wavelength. *Acta Sin. Quantum Opt.* **2017**, *23*, 99.
36. Gao, Y.; Feng, J.; Li, Y.; Zhang, K. Generation and Measurement of Squeezed Vacuum States at Audio-Band Frequencies. *Appl. Sci.* **2019**, *9*, 1272. [[CrossRef](#)]
37. Sun, X.; Wang, Y.; Tian, L.; Shi, S.; Zheng, Y.; Peng, K. Dependence of the squeezing and anti-squeezing factors of bright squeezed light on the seed beam power and pump beam noise. *Opt. Lett.* **2019**, *44*, 1789–1792. [[CrossRef](#)]
38. McKenzie, K.; Mikhailov, E.E.; Goda, K.; Lam, P.K.; Grosse, N.; Gray, M.B.; Mavalvala, N.; McClelland, D.E. Quantum noise locking. *J. Opt. B Quantum Semiclassical Opt.* **2005**, *7*, S421–S428. [[CrossRef](#)]
39. Chelkowski, S.; Vahlbruch, H.; Danzmann, K.; Schnabel, R. Coherent control of broadband vacuum squeezing. *Phys. Rev. A* **2007**, *75*, 043814. [[CrossRef](#)]
40. Fu, G.; Cao, Y.; Wang, Y.; Wan, Y.; Wang, L.; Li, C. Dynamic Phase Measuring Profilometry Based on Tricolor Binary Fringe Encoding Combined Time-Division Multiplexing. *Appl. Sci.* **2019**, *9*, 813. [[CrossRef](#)]
41. Chow, C.W.; Ellis, A.D.; Parmigiani, F. Time-division-multiplexing using pulse position locking for 100 Gb/s applications. *Opt. Express* **2009**, *17*, 6562–6567. [[CrossRef](#)]
42. Jin, X.; Su, J.; Zheng, Y.; Chen, C.; Wang, W.; Peng, K. Balanced homodyne detection with high common mode rejection ratio based on parameter compensation of two arbitrary photodiodes. *Opt. Express* **2015**, *23*, 23859. [[CrossRef](#)]
43. Zhou, H.; Wang, W.; Chen, C.; Zheng, Y.; Low-Noise, A. Large-Dynamic-Range-Enhanced Amplifier Based on JFET Buffering Input and JFET Bootstrap Structure. *IEEE Sens.* **2015**, *15*, 2101. [[CrossRef](#)]
44. Zhou, H.; Yang, W.; Li, Z.; Li, X.; Zheng, Y. A bootstrapped, low-noise, and high-gain photodetector for shot noise measurement. *Rev. Sci. Instrum.* **2014**, *85*, 013111. [[CrossRef](#)]
45. Li, Z.; Sun, X.; Wang, Y.; Zheng, Y.; Peng, K. Investigation of residual amplitude modulation in squeezed state generation system. *Opt. Express* **2018**, *26*, 18957. [[CrossRef](#)]
46. Li, Z.; Ma, W.; Yang, W.; Wang, Y.; Zheng, Y. Reduction of zero baseline drift of the Pound-Drever-Hall error signal with a wedged electro-optical crystal for squeezed state generation. *Opt. Lett.* **2016**, *41*, 3331. [[CrossRef](#)]
47. Jia, X.; Yan, Z.; Duan, Z.; Su, X.; Wang, H.; Xie, C.; Peng, K. Experimental realization of three-color entanglement at optical fiber communication and atomic storage wavelengths. *Phys. Rev. Lett.* **2012**, *109*, 253604. [[CrossRef](#)]
48. Su, X.; Zhao, Y.; Hao, S.; Jia, X.; Xie, C.; Peng, K. Experimental preparation of eight-partite cluster state for photonic qumodes. *Opt. Lett.* **2012**, *37*, 5178. [[CrossRef](#)]
49. Sun, X.; Wang, Y.; Tian, L.; Zheng, Y.; Peng, K. Detection of 13.8 dB squeezed vacuum states by optimizing the interference efficiency and gain of balanced homodyne detection. *Chin. Opt. Lett.* unpublished.

